Journal of Fluids and Structures (2000) **14,** 1071–1088
doi:10.1006/jfls.2000.0308, available online at http://www.idealibrary.com on IDEAL®

ADDED MASS AND OSCILLATION FREQUENCY FOR A CIRCULAR CYLINDER SUBJECTED TO VORTEX-INDUCED VIBRATIONS AND EXTERNAL DISTURBANCE

K. VIKESTAD
MARINTEK A/S, P.O.Box 4125 Valentinlyst
N-7450 Trondheim, Norway

J. K. VANDIVER
Department of Ocean Engineering, Massachusetts Institute of Technology
Cambridge, MA 02139, U.S.A.

AND

C. M. LARSEN
Department of Marine Structures, Norwegian University of Science and Technology
N-7491 Trondheim, Norway

(Received 12 February 1999, and in final form 12 May 2000)

This paper reports results from an experiment with a lightly damped elastically mounted rigid cylinder subjected to constant flow velocity. The cylinder was allowed to vibrate in the cross-flow direction and was fixed in the flow direction. The Reynolds numbers varied from 10^4 to 6×10^4. The added mass for the freely vibrating cylinder agreed well with the results found by others in driven cylinder tests. The predicted natural frequency based on the measured added mass was approximately equal to the measured mean oscillation frequency. The added mass calculated from one oscillation cycle to the next varied considerably. The oscillation frequency from one oscillation to the next corresponded to the natural frequency including the added mass for the same cycle. By movement of the attachment point of the elastic members to the external structure a disturbance could be added to the normal vortex-induced vibrations (VIV) response. When an external disturbance was introduced at a frequency other than the VIV frequency, the added mass coefficient was found to be weakly influenced by the external harmonic disturbance.

1. INTRODUCTION

THE PREDICTION OF THE RESPONSE FREQUENCIES of flexible marine risers in sheared flows is important in the estimation of fatigue damage rates. Response frequencies depend on both the natural frequencies of the structure and the distribution of vortex-shedding frequencies along the riser. The natural frequencies depend on the added mass distribution along the riser. The excitation frequency components depend on the velocity profile and local cylinder motion. The local cylinder motion typically has many frequency components. Little is known about the effect of multiple frequency motion components on added mass coefficients or excitation force amplitudes and frequencies. The experiments described in this

0889–9746/00/101071 + 18 $35.00/0

paper were intended to begin the investigation of vortex-induced vibration (VIV) in a multiple frequency environment.

A preliminary estimate of the response frequency of an elastically mounted cylinder excited by vortex shedding may be based on knowledge of the Strouhal number (St) where the estimate of the vortex-shedding frequency, f_s is given by

$$f_s = \mathrm{St}\frac{U}{D}; \tag{1}$$

U is the flow velocity and D is the cylinder diameter. The Strouhal number for fixed cylinders is approximately 0·2 for a wide range of subcritical Reynolds numbers (Re) between 10^3 and 10^5. For $10^5 < \mathrm{Re} < 2 \times 10^6$ the Strouhal number generally increases, but with wide variations in the data.

For cylinders elastically mounted in the cross-flow direction, the vortex-shedding frequency may be altered by the lock-in phenomenon in which resonant motion of the cylinder at its natural frequency controls the frequency of vortex shedding.

In the sub-critical Reynolds number range, this often leads to a lower vortex-shedding frequency than that for a fixed cylinder.

The relationship between VIV response and the system natural frequency is reflected in another dimensionless parameter, the reduced velocity (U_r) given by

$$U_r = \frac{U}{f_n D}. \tag{2}$$

The complication which arises in the use of this parameter is that the natural frequency (f_n) is not constant but depends upon the fluid added mass of the cylinder. The oscillation frequency, and thereby probably also the added mass, is known to be dependent on the reduced velocity for small mass ratio cylinders (Sarpkaya 1979). This leads to a circular problem which is most commonly resolved by fixing the definition of the natural frequency when computing the reduced velocity. In this paper, the reduced velocity is based on the value of the natural frequency measured in still water, and corresponds to an added mass coefficient of 1·04.

In this paper the, relationship between added mass and response frequency is investigated for an elastically mounted cylinder in fluid flow. Experimental results are presented which reveal that, even under uniform flow conditions, there are significant cycle-to-cycle variations in added mass and vibration period. It is also shown that the added mass is influenced by the addition of cylinder motion components at frequencies which are different from the natural vortex-induced vibration response. This results in cylinder motion with more than one-frequency component. Knowledge of added mass in a multi-frequency environment is important for predicting multi-mode VIV response of risers and cables in sheared flow.

2. DESCRIPTION OF THE EXPERIMENT

2.1. The Apparatus

The experimental apparatus is shown in Figure 1. The 2 m long and 10 cm diameter rigid cylinder was horizontally mounted in a hinged framework. The intention was that the cylinder should be able to have translatory motion in the cross-flow direction, but be restrained from motion in other directions. The structural damping was kept as low as possible by using ball bearings in the hinges. End-effects were minimized by means of end-plates. The diameter of the end-plates was five times the cylinder diameter. The mass

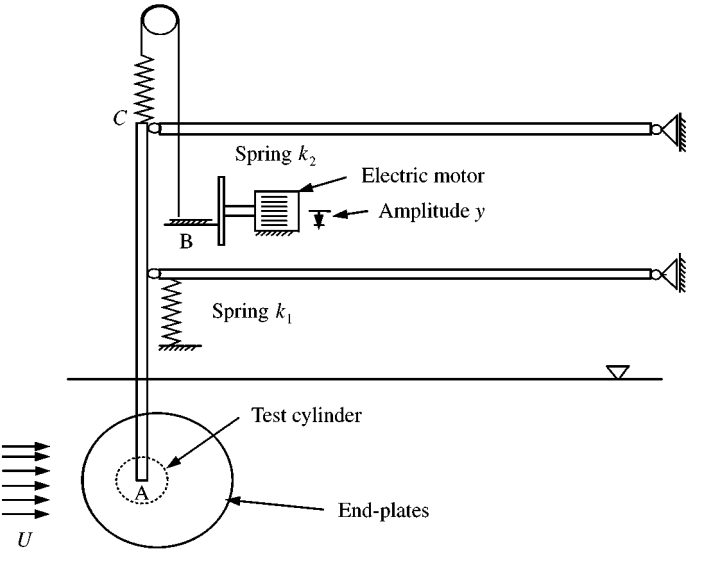

Figure 1. Schematic drawing of the experimental apparatus.

ratio $m/\rho D^2 = 1{\cdot}3$ includes the effect of all moving parts of the system. The mass ratio was intended to represent realistic marine risers and therefore both the framework and the test cylinder were made of aluminium. The flow was in the stable sub-critical regime, Re from 10^3 to 10^5. The properties of the apparatus are given in Table 1. The upper spring support was connected to a fixed displacement scotch yoke oscillator. The oscillator gave the support an harmonic motion with a specified amplitude and frequency. The damping ratio was found by averaging the results from several decay tests. The apparatus was placed on a carriage in a 25 m long $\times$ 2·5 m wide towing tank at NTNU, Trondheim. The mean position of the cylinder was 0·6 m below the surface in the 1·2 m deep tank. The carriage motor was controlled by a variable frequency power supply and gave the carriage an acceleration of approximately 0·6 m/s^2. For a reduced velocity of 6 ($U_r = U/(f_0 D)$), based on the natural frequency in still water, constant flow velocity was reached in $\frac{1}{4}$ of a natural period. A thorough description of the experiment is found in Vikestad (1998).

2.2. Experiments Conducted

In this paper results from two kinds of experiments are given.

(i) *No support excitation*: An elastically mounted cylinder was towed without support excitation. U_r was varied from 2·8 to 13·2 with 23 different reduced velocities. Each series of tests was done three times to check the repeatability. In this paper the three series are named First, Second, and Third when referred to. The first series was done before the external excitation tests, and the third series was done after.

(ii) *With external excitation*: At the same reduced velocities as above, the cylinder was subjected to a support motion. Three different support amplitudes (2, 4, and 6 cm) were used, combined with 12 different frequencies, varying from approximately $0{\cdot}5f_0$ to $2{\cdot}0f_0$. The total number of runs for this case was 828 (23 velocities $\times$ 3 support amplitudes $\times$ 12 support frequencies = 828).

TABLE 1

The properties of the apparatus

Cylinder length	L	2·00	m
Cylinder diameter	D	10·0	cm
Total stiffness	k_{tot}	415	N/m
Stiffness of oscillator support	k_2	266	N/m
Cylinder volume	V_{cyl}	0·0157	m^3
Natural frequency in air	f_{air}	0·634	Hz
Natual frequency in still water	f_0	0·497	Hz
Effective dry mass	m	26·12	kg
Effective wet mass		42·5	kg
Added mass coefficient at f_0		1·04	
Mass ratio		1·306	
Specific gravity		1·664	
Damping ratio, $\zeta = c/c_{crit}$)			
in air		0·07–0·1	%
in water, no cylinder		0·7–1·0	%
in water with cylinder (Amplitude/D) $< 0·25$		1·5	%

The results of each experiment were time series of cylinder displacement, acceleration, and total cylinder end forces. The fluid force on the cylinder in the cross-flow direction (F_v) was found by removing the part due to inertia of the cylinder from the measured forces at the end of the cylinder.

For the experiments with support motion, time series for the support displacement, acceleration, and spring force were also found.

3. CALCULATION OF ADDED MASS

The oscillatory system can be described by the dynamic equilibrium equation

$$m\ddot{x} + c\dot{x} + k_{tot}x = F_v(t) + k_2 y(t), \tag{3}$$

where m is the dry mass of the cylinder, and c the structural damping coefficient; F_v is the cross-flow component of the total hydrodynamic force, x is the cylinder motion, and y is the motion of the support system. If the response is assumed to be periodic with a principal harmonic $x(t) = x_0 \sin(\omega t)$, we may assume that the principal harmonic component of F_v is given by $F_v = F_0 \sin(\omega t + \phi)$. Using the known properties

$$F_0 \sin(\omega t + \phi) = F_0 \cos\phi \sin(\omega t) + F_0 \sin\phi \cos(\omega t), \tag{4}$$

this fluid force may be split into two components, one in phase with the cylinder acceleration and the other with velocity:

$$\left(m + \frac{F_0 \cos\phi}{\omega^2 x_0}\right)\ddot{x} + \left(c - \frac{F_0 \sin\phi}{\omega x_0}\right)\dot{x} + k_{tot}x = k_2 y(t). \tag{5}$$

Using the relationships

$$\lim_{T\to\infty} \frac{\int_t^{t+T} F_v \dot{x}\,dt}{T} = \frac{1}{2}\omega x_0 F_0 \sin\phi \tag{6}$$

and

$$\lim_{T\to\infty}\frac{\int_t^{t+T}F_v\,\ddot{x}\,\mathrm{d}t}{T} = -\frac{1}{2}\omega^2 x_0 F_0\cos\phi, \tag{7}$$

equation (5) can be written as

$$\left(m-\lim_{T\to\infty}\frac{2}{T(\omega^2 x_0)^2}\int_t^{t+T}F_v\,\ddot{x}\,\mathrm{d}t\right)\ddot{x} + \left(c-\lim_{T\to\infty}\frac{2}{T(\omega x_0)^2}\int_t^{t+T}F_v\,\dot{x}\,\mathrm{d}t\right)\dot{x} + k_{\mathrm{tot}}x = k_2 y(t). \tag{8}$$

The $\ddot{x}$ term in equation (8) provides a means of estimating the added mass coefficient from experimental data. An approximation to the averaging integral in equation (8) is found by integrating over an integer number (n) of oscillation periods. The added mass coefficient (C_a) may be estimated from

$$C_a = -\frac{8}{nT\rho\pi D^2 L(\omega^2 x_0)^2}\int_t^{t+nT}F_v\ddot{x}\,\mathrm{d}t. \tag{9}$$

For the runs without support motion, equation (9) was used both for calculating an average C_a over many periods and for calculating a time-dependent C_a, by averaging over a sequence of single periods.

For the runs with support motion the experimental data were filtered into two frequency regimes:

(i) a narrow band around the support motion frequency; This is defined as support-induced motion, whether or not it controlled the vortex-shedding frequency;

(ii) all frequencies outside the band centered on the support motion frequency; Since this was not oscillation due to support motion, it was defined as vortex-induced vibration, VIV.

The use of equation (9) is demonstrated in Figures 2 and 3. Figure 2 is the time series for cylinder acceleration. Figure 3 presents the product of the cylinder acceleration and the total hydrodynamic force in the cross-flow direction for one of the three tests with $U_r = 8{\cdot}0$. When the product $F_v\ddot{x}$ is positive, the added mass coefficient is negative, according to equation (9). Figure 3 clearly shows that the added mass coefficient is not constant, as this product changes from positive to negative values. The acceleration amplitude $\omega^2 x_0$ as used in equation (9) was found from the measured root-mean-squared (r.m.s.) value of acceleration multiplied by $\sqrt{2}$.

4. RESULTS AND DISCUSSION

4.1. Mean Added Mass for VIV without Support Motion

The added mass coefficient estimated using equation (9) as a function of reduced velocity is given in Figure 4(a). The figure shows the results for the three repeated series of tests and clearly illustrates that the results are reproducible. The added mass coefficient equals 1·0 for U_r close to 5·5, and 0·0 for U_r near 8. For higher reduced velocities, $C_a < 0{\cdot}0$. In Figure 4(b) the sloped line of data points are the mean oscillation frequency normalized by the still water natural frequency, plotted against the reduced velocity. The mean oscillation frequency is found from $\sqrt{(\ddot{x}_{\mathrm{rms}}/x_{\mathrm{rms}})}/(2\pi)$. There is no evidence that the oscillation frequency is locked-in to one fixed natural frequency as has been frequently seen from experiments with very high mass ratio, e.g. in air.

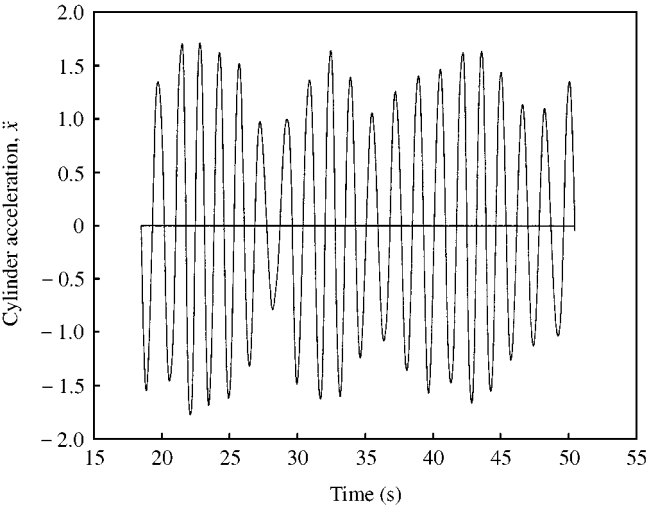

Figure 2. Cylinder acceleration versus time for $U_r = 8{\cdot}0$, no support motion.

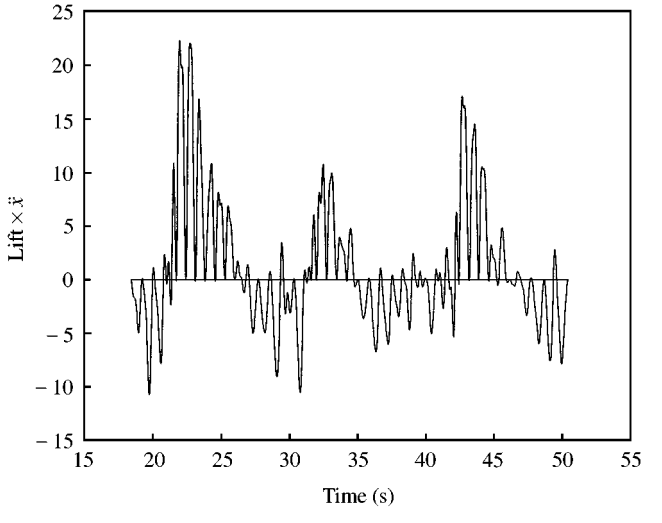

Figure 3. Total hydrodynamic force in cross-flow direction multiplied by the cylinder acceleration versus time for $U_r = 8{\cdot}0$ (same run as Figure 2, no support motion). This is the $F_v\ddot{x}$ term in equation (9).

In fact, over a wide range of reduced velocities the oscillation frequency is the true natural frequency $f_n(U_r)$, where we define the true natural frequency as

$$f_n(U_r) = \frac{1}{2\pi}\sqrt{\frac{k_{\text{tot}}}{m + \rho V_{\text{cyl}} C_a(U_r)}}. \tag{10}$$

This is illustrated by the horizontal line of data points in Figure 4(b) which is the measured oscillation frequency divided by $f_n(U_r)$. In other words, the added mass coefficient decreases monotonically with reduced velocity, resulting in a natural frequency which increases with reduced velocity, as reported by numerous papers (Anand 1985; Kozakiewicz *et al.*, 1994; Sumer & Fredsøe 1997).

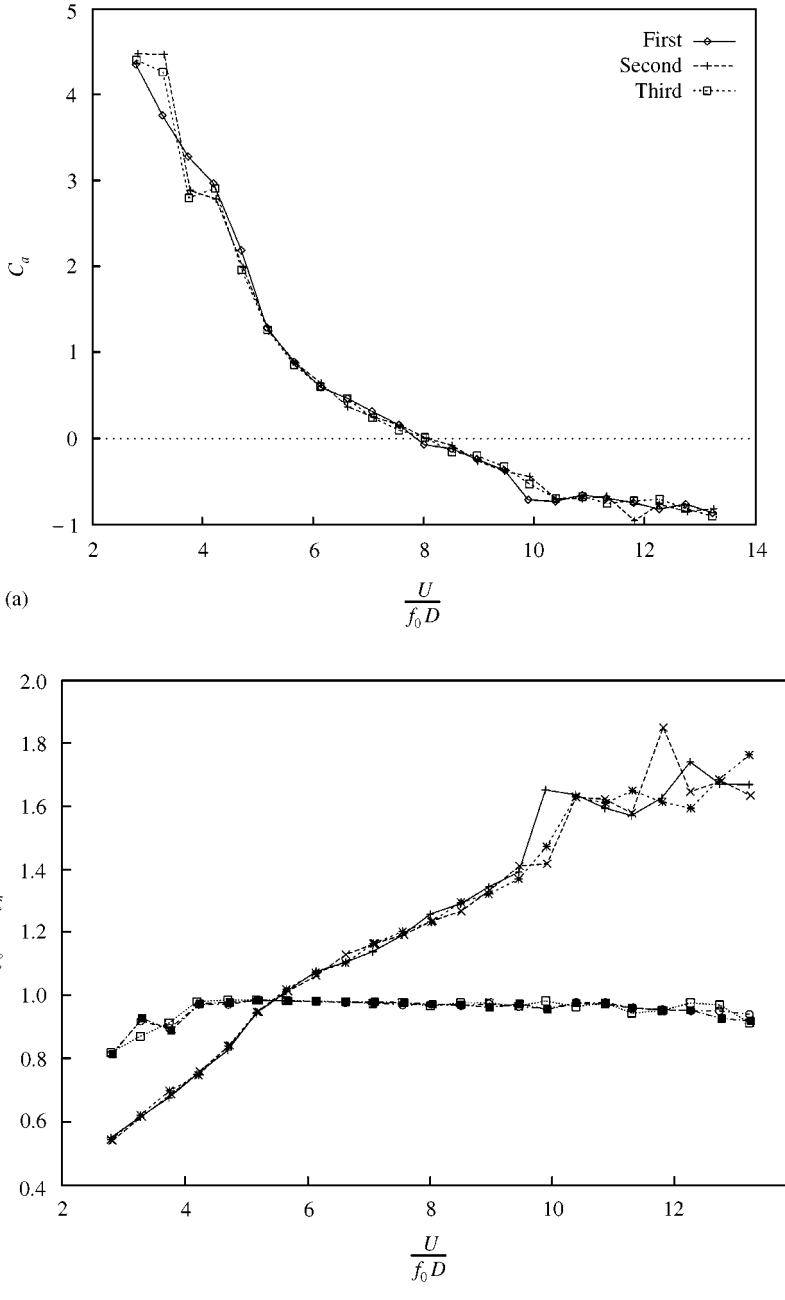

Figure 4. (a) Added mass and (b) frequency results for towing without support excitation. Specifically, (b) shows the mean oscillation frequency divided by natural frequency in still water (0·497 Hz) (sloped lines) and the mean oscillation frequency divided by the true natural frequency using the added mass from Figure 4(a) corresponding to the given reduced velocity (the horizontal lines).

This has the consequence that low mass ratio cylinders have lock-in regions that extend over a broader range of flow speeds than do high mass ratio cylinders as described in Vandiver (1993). This effect is illustrated in Figures 4(a) and 4(b). In Figure 4(a) the added mass coefficient is shown to decrease as the reduced velocity increases. In this paper, reduced velocity is defined in terms of a fixed natural frequency; in this case that was

measured in still water. Once lock-in commences, at approximately $U_r = 4$, then the natural frequency of the cylinder increases with increasing reduced velocity, enabling lock-in to persist, in this case up to approximately $U_r = 12$, because the mass ratio is quite low ($m/\rho D^2 = 1{\cdot}3$). High mass ratio cylinders have much narrower lock-in ranges, because the variation in added mass results in a smaller increase in the natural frequency. If reduced velocity were defined in terms of the true natural frequency, then cylinders with different mass ratios would appear to have similar width lock-in regions extending from approximately 5–8 in reduced velocity. However, for purposes of reporting experimental data, it is better to express reduced velocity using a fixed value of natural frequency. Variability of the oscillation frequency with reduced velocity was also shown by Anand (1985) in his doctoral thesis. Using higher mass ratio ($m/\rho D^2 = 4{\cdot}5$) the oscillation frequency did not vary as much as shown in the present investigation.

The net power loss due to friction was very low in these experiments and the results may be compared with other lightly damped systems such as Gopalkrishnan (1993). Lift coefficients and added mass coefficients from his study are plotted in Figure 5 as a function of nondimensional frequency ratio, defined as $\hat{f} = f_{\text{osc}} D/U$. His results were obtained from a forced oscillation experiment. The results may be compared to the results presented in this paper under similar conditions of lift force. Since the damping was very small in our experiments, then at dynamic equilibrium the lift coefficient in phase with velocity is very small. This condition is approximated by the zero lift coefficient contours in Figure 5(a). We have transferred this contour to the added-mass plot in Figure 5(b). From this we can extract added mass coefficients at each value of frequency ratio along the zero lift coefficient contour. We must also convert the frequency ratio $\hat{f}$ to reduced velocity defined with a constant natural frequency as observed in still water. This was done by inserting into equation (11) the added mass values taken from the zero lift contours in Figure 5(b),

$$U_r = \frac{1}{\hat{f}} \sqrt{\frac{m + 1{\cdot}0\rho V_{\text{cyl}}}{m + C_a \rho V_{\text{cyl}}}}. \tag{11}$$

The added mass coefficient found from the lift coefficient in phase with acceleration is also given by Gopalkrishnan (1993, eq. 3.8):

$$C_a = -\frac{1}{2\pi^3} \frac{C_{L_A}}{A/D\hat{f}^2}, \tag{12}$$

where C_{L_A} is the lift coefficient in phase with cylinder acceleration. Thus there are two ways of extracting data from Gopalkrishnan [directly from Figure 5(b) or by using the plot for lift coefficient in phase with acceleration, C_{L_A}, and equation (12)]. They give nearly identical results, as shown in Figure 6. In Figure 6 the results from the present investigation are compared to results from Vikestad *et al.* (1997) (which used the same apparatus with different mass ratio and tow velocities) and the coefficients extracted from Gopalkrishnan's experiments. The plot reveals that the added mass coefficients found by free oscillation tests and forced oscillation tests agree very well. For very low reduced velocities, the acceleration amplitudes are very small, and the coefficient is very sensitive to small errors in the measurements. Thus, the very high added mass coefficients found for low reduced velocities have considerable uncertainty. There are small differences, especially for the important U_r-range between 5 and 7 where the freely oscillating system has slightly lower added mass than the driven cylinder. This may be due differences in the amplitudes of motion. While the zero-lift curve of Figure 5(a) corresponded to a maximum response of 0·82 A/D (A is the mean cylinder amplitude of response), the free vibration maximum response was 1·15 A/D. Also differences in Reynolds number may be a source of difference as Gopalkrishnan's were

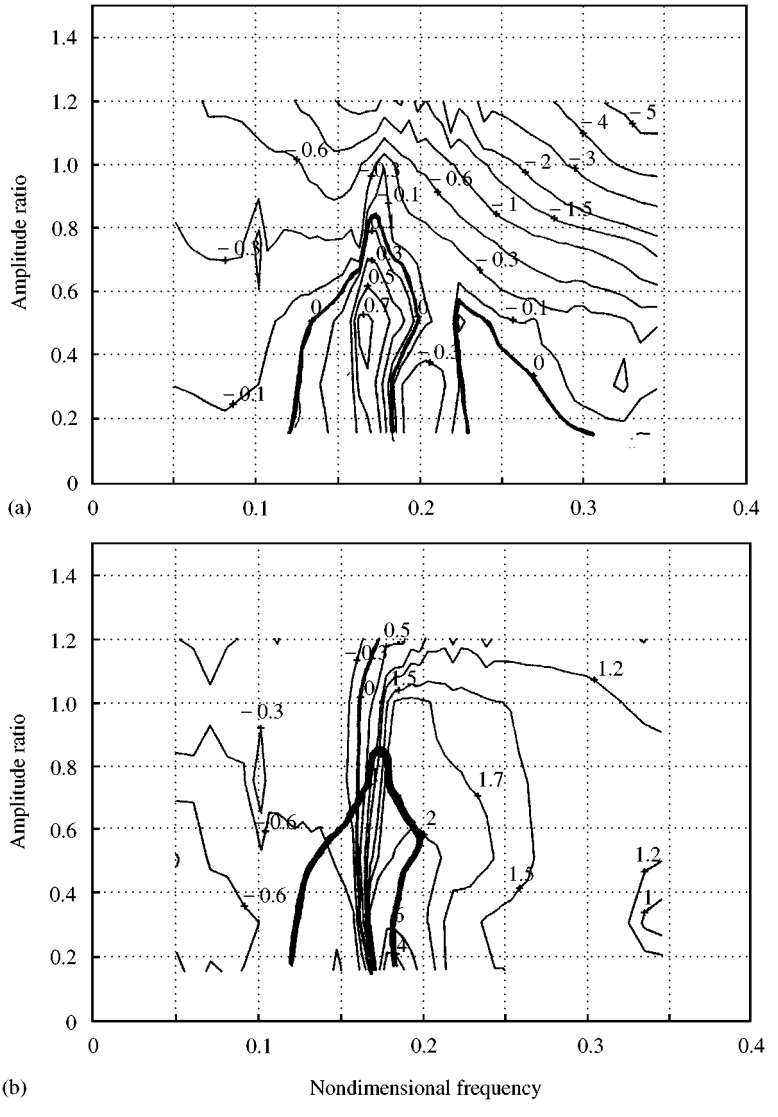

Figure 5. Results from the driven cylinder experiments of Gopalkrishnan (1993) (printed with permission from MIT). (a) Contours of the lift coefficient in phase with velocity (Figure 3–14 in Gopalkrishnan's thesis). (b) Contours of the added mass coefficient, with the contour for zero lift in phase with velocity added (Figure 3–16 in Gopalkrishnan's thesis).

approximately $\mathrm{Re} \approx 10^4$ and the free vibration experiments described here were from $1{\cdot}4 \times 10^4$ to $6{\cdot}5 \times 10^4$. Free surface or bottom effects may have influenced the results. One final explanation of the difference in amplitude is the possibility of phase angle errors in the measurement of the measured forces. A 1° difference in phase angle would account for the difference in results for the response amplitude, which correspond to zero lift force.

4.2. Time Variability of Added Mass, without Support Motion

The mean added mass as a function of reduced velocity was given in the previous section. In this section the variation of the added mass from one vibration cycle to the next is

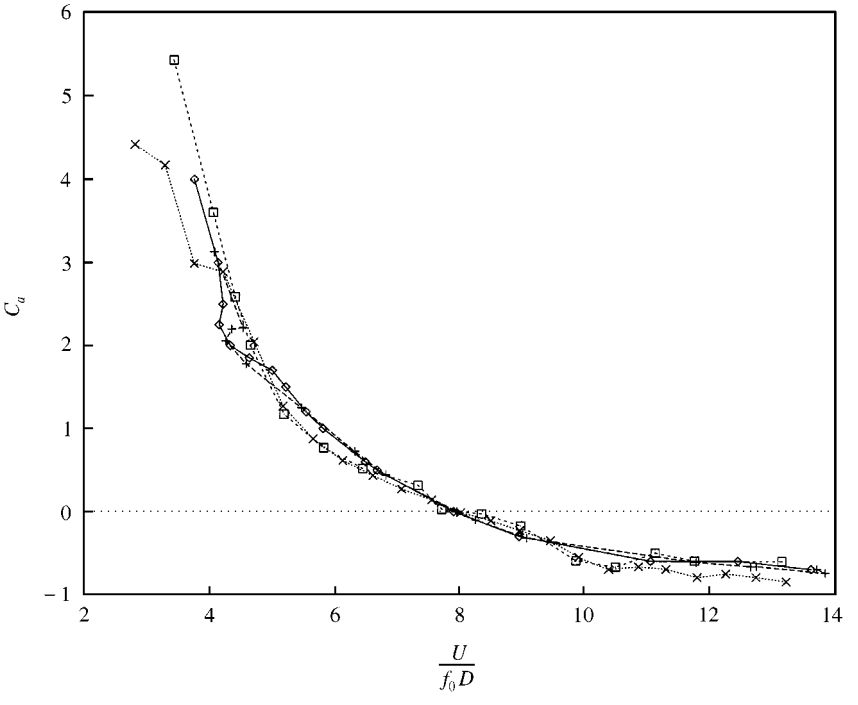

Figure 6. Comparison between added mass coefficients: —◇—, Gopalkrishnan, C_a; --- +---, Gopalkrishnan, C_{L_A}; ---□---, Vikestad *et al.* (1997); ---- × ----, Present. The results of Gopalkrishnan for zero mean lift (mean power is zero) are found from the contour plots of the added mass coefficient and the lift coefficient in phase with acceleration.

investigated. When calculating the added mass, equation (9) was used. The number of oscillation periods in the integral was reduced to one. A time-averaged added mass over each oscillation period of the run was found. The acceleration amplitude needed in equation (9) was computed from the r.m.s. acceleration as follows: $\omega^2 x_0 = \ddot{x}_0 = \sqrt{2}\,\mathrm{SD}(\ddot{x})$ (SD = standard deviation). The time window, which was one period long, both started and ended with zero displacement. Figure 2 shows the time series for the acceleration and Figure 3 shows the lift force times the acceleration for a reduced velocity $U_r = 8{\cdot}0$. (The plot is from the first of the three runs at $U_r = 8{\cdot}0$.) From the figure one can see that the added mass is *not* constant during the tow. When $F_v\ddot{x}$ is positive in Figure 3, the added mass coefficient is negative and *vice versa*. Some questions arise concerning this variation of added mass, as follows.

How large are the variations? If the variations are small, the change of oscillation frequency due to this variation is limited.

Are the variations systematic in any way? As shown earlier, the mean added mass for a given reduced velocity is fairly deterministic. Do the variations also follow a predictable pattern?

How does the oscillation frequency vary? The mean frequency of oscillation has been shown to correspond to the natural frequency computed using the mean added mass, see equation (10). Is there a similar relation between the frequency of oscillation and added mass when both are estimated from a single period of motion?

Figure 7 shows the displacement time history for the first run at a reduced velocity of 8·0. It also shows a plot of the time-dependent added mass for the same run, computed using equation (9), but integrating over single periods of oscillation. The transient start-up of the

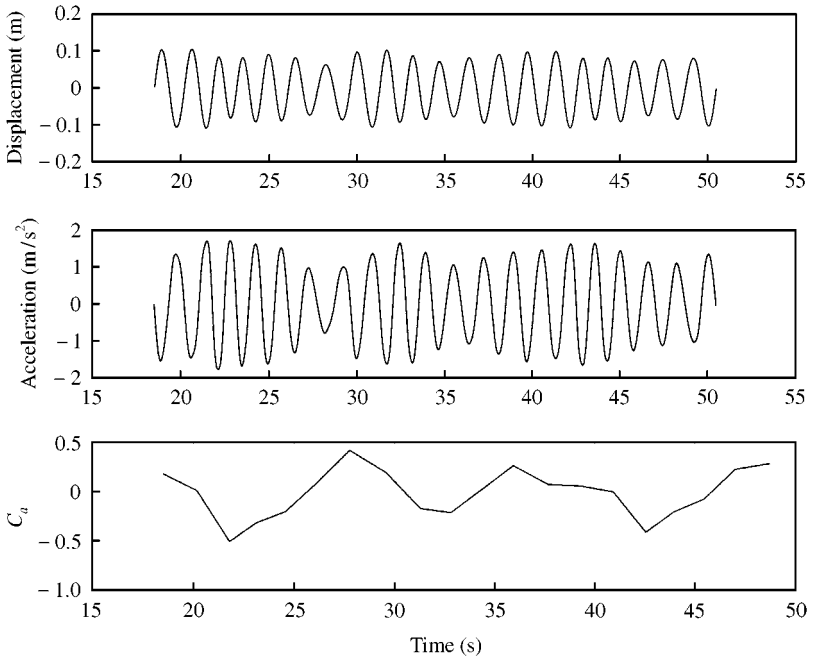

Figure 7. Time series for the cross-flow displacement, acceleration, and time-variable added mass coefficient for the first of the three tests at $U_r = 8{\cdot}0$.

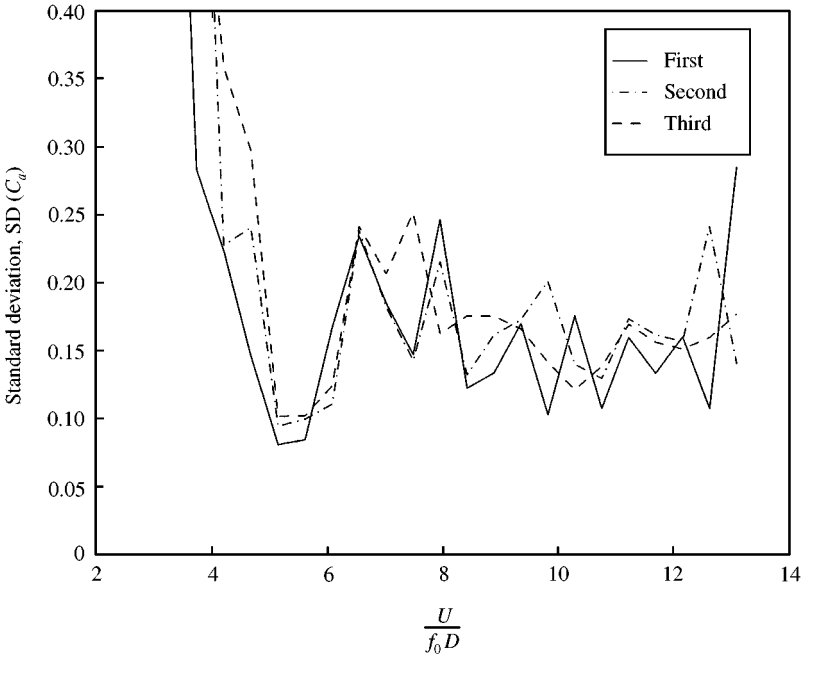

Figure 8. Standard deviation of the added mass coefficient versus reduced velocity.

run has been excluded from the analysis. The time-varying added mass described above has been computed one period at a time. From the inverse of time periods we can estimate an up-crossing frequency and compare it to the natural frequency which can be predicted using the added mass estimated for that period. The result is shown in Figure 9. In the figure, both predicted and measured frequency have been normalized by the mean oscillation frequency over the whole run. The difference between predicted and measured frequency was less than 3·5% for all cases, demonstrating that both added mass and natural frequency change in a consistent manner from one period to the next. Figure 8 shows the standard deviation (SD) of C_a as a function of U_r for the three different tests. In Figure 10(a) the mean $\pm$ one standard deviation of added mass are plotted as a function of reduced velocity. The largest variation is below 4 in U_r. In Figure 10(b) the predicted variation in natural frequency corresponding to the measured changes in added mass is presented. The period-to-period variation in natural frequency is shown for plus and minus one standard deviation of added mass. The extreme values are also shown, corresponding to the maximum and minimum values of the measured added mass.

Figure 10(a) indicates the relative variation of the added mass coefficient. For each of the three towing tests with identical (and constant) reduced velocity, the added mass coefficient maximum, minimum and $\pm$ standard deviation was calculated. "*Maximum*" denotes the mean of the three maximum values for added mass found for the three runs at each reduced velocity. "*Minimum*" is the mean of the three minimum values. The mean value of the added mass coefficients over all three runs at a given reduced velocity was calculated and plotted in Figure 10(a) with the label "*Mean*". For the "*Mean* $\pm$ SD", the mean of the three values for the standard deviation found in Figure 8 is added/subtracted from the mean C_a. It is clear from the figure that the variation of the added mass coefficient is very small for $U_r = 4{\cdot}5$–6. The effect on the "variable natural frequency", computed using the added mass values found from Figure 10(a), relative to the mean natural frequency, is given in Figure 10(b). Here we see that for U_r from 4 to 6, the variations of vibration frequency is less than $\pm$ 5%. For smaller and larger U_r, the variations are 10% or greater.

4.3. Correlation between Added Mass and Displacement

Testing the relationship between two variables x and y by means of the *correlation coefficient* ρ is given as

$$\rho(x, y) = \frac{(1/n)\sum_{i=1}^{n}(x_i - \bar{x})(y_i - \bar{y})}{\mathrm{SD}(x)\mathrm{SD}(y)}. \tag{13}$$

Let x_i be the added mass coefficient estimated for each period (i) of the motion. Let y_i be the corresponding r.m.s. displacement; $\bar{x}$ and $\bar{y}$ are the mean added mass and r.m.s. displacement over the run. Figure 11 shows the correlation between the added mass coefficient and cylinder displacement. There is strong correlation between reduced velocities of 4–6. The coefficient switches sign at $U_r \approx 5$. Outside of this range the correlation is much lower.

The effect of the variable added mass on the natural frequencies of long cables or risers in sheared flow is not well understood. In modal analysis, the modal mass is found by integrating over the length of the riser the product of the mass per unit length and the square of the mode shape. It may be that the local time variations in added mass revealed in this study may be averaged out by the integration over the length of the riser and will give a more or less constant modal mass and steady values for natural frequencies. It may on the other hand be that the variation in added mass may be sufficient to cause frequent changes

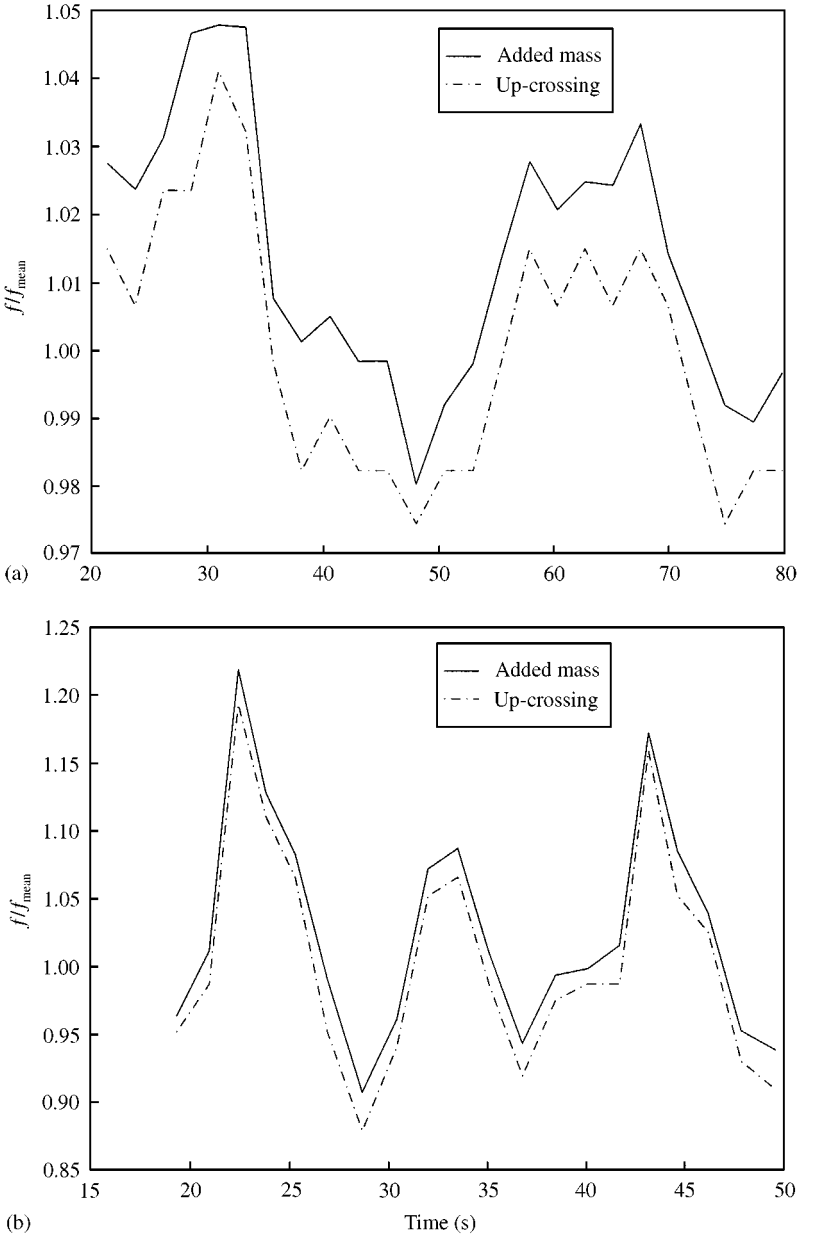

Figure 9. Observed oscillation frequency and calculated natural frequency based on added mass for the same cycle reduced velocity. Frequencies are normalized using the mean oscillation frequency. (a) Frequency variations at $U_r = 4{\cdot}7$; (b) at $U_r = 8{\cdot}0$.

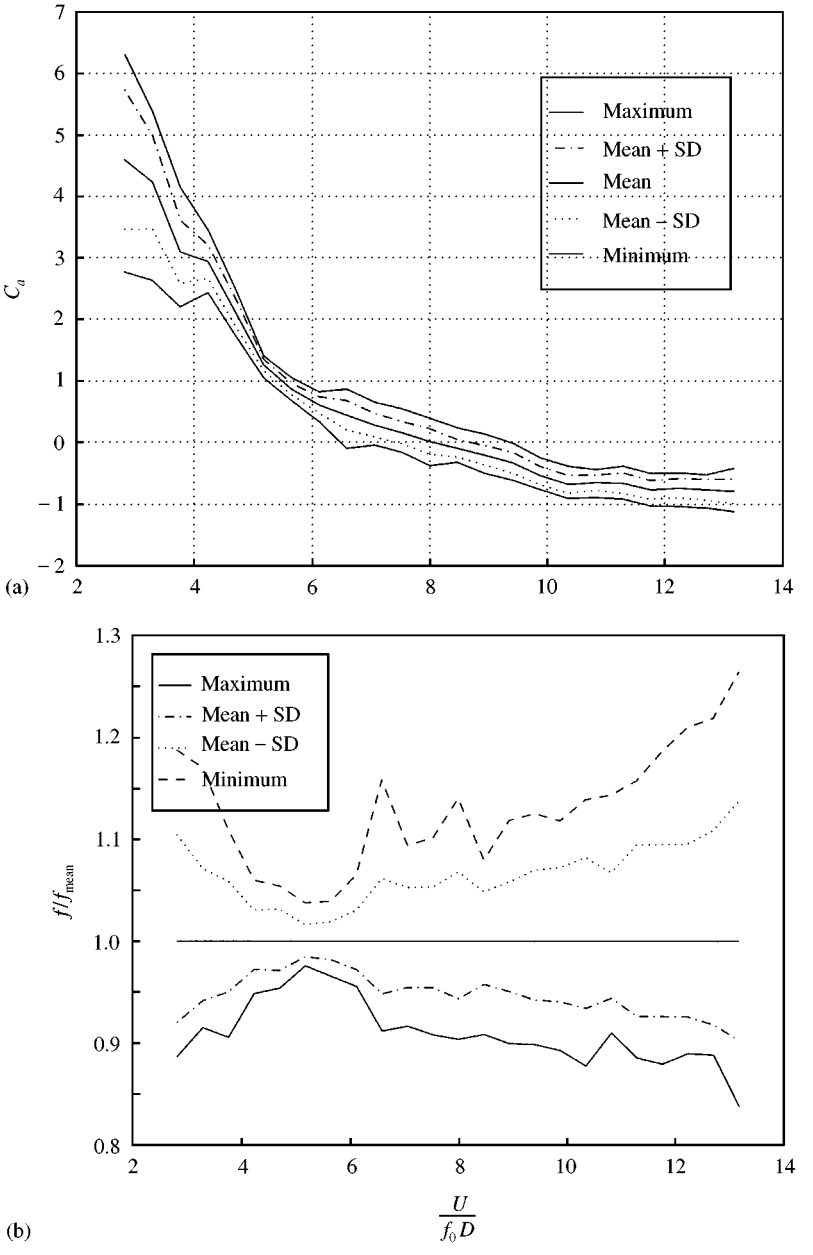

Figure 10. (a) The time-variable added mass, and its effect on the natural frequency. For a given reduced velocity, the results in the plot are the mean of the results found using the three different tests, e.g. the "maximum" means the mean of the three results for the maximum added mass for the tests. In (b) time-variable natural frequency inferred from different values of added mass. The results are normalized with the natural frequency found using the mean added mass coefficient at each reduced velocity.

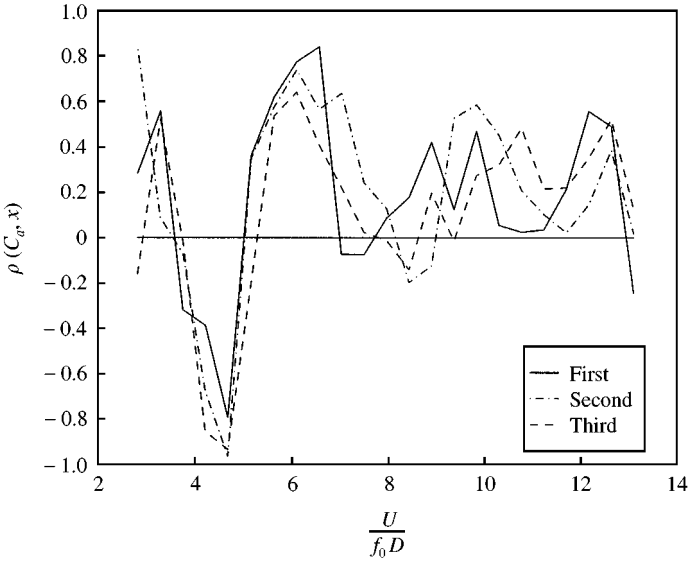

Figure 11. Correlation coefficient between the variable added mass and the cylinder displacement amplitude.

in natural frequencies and frequent changes in observed response from one mode to another.

4.4. Behavior of Added Mass in the Presence of an Outside Disturbance

A set of experiments were conducted to simulate vibration at one location of a long cable due to VIV at another location on the cable with different flow velocity and different vortex-shedding frequency. The motion frequency introduced by the support motion (f_{ex}) simulated the vibration caused by VIV at a different location. The test cylinder was also allowed to respond to vortex-related lift forces (frequency f_v). When the support motion and VIV frequencies were different it was possible to estimate from the measurements the added mass coefficient associated with the VIV response frequency by using equation (9). The frequency components of the support motion were filtered out from the lift force and the acceleration measurements using a frequency-domain narrow-band filter, centred on the support frequency.

Contour plots of the estimated added mass coefficient at the VIV frequency f_v are given in Figures 12–14. There is one plot for each of the three support motion amplitudes. At zero frequency in still water static support motion amplitudes of 2, 4, and 6 cm caused $0{\cdot}128A/D$, $0{\cdot}256A/D$, and $0{\cdot}385A/D$ static displacements of the cylinder. The horizontal axis in the figures is the reduced velocity based on the natural frequency in still water. The vertical axis is the ratio of the support motion frequency f_{ex} to the VIV frequency observed without support motion f_{osc}, see Figure 4(b). The contours for added mass equal to 0·0 and 1·0 are marked with thick, approximately vertical lines. Negative added mass is noted with dashed lines. The very thick lines mark the "disturbance controlled VIV" region. This region is defined by the frequency ratio

$$f_{\text{ratio}} = \left(\frac{\ddot{x}_{\text{cyl}_{\text{rms}}}}{x_{\text{cyl}_{\text{rms}}}}\right)^{1/2}\left(\frac{\ddot{x}_{\text{sup}_{\text{rms}}}}{x_{\text{sup}_{\text{rms}}}}\right)^{-1/2} = \frac{f_{\text{sup}}}{f_{\text{ex}}}, \tag{14}$$

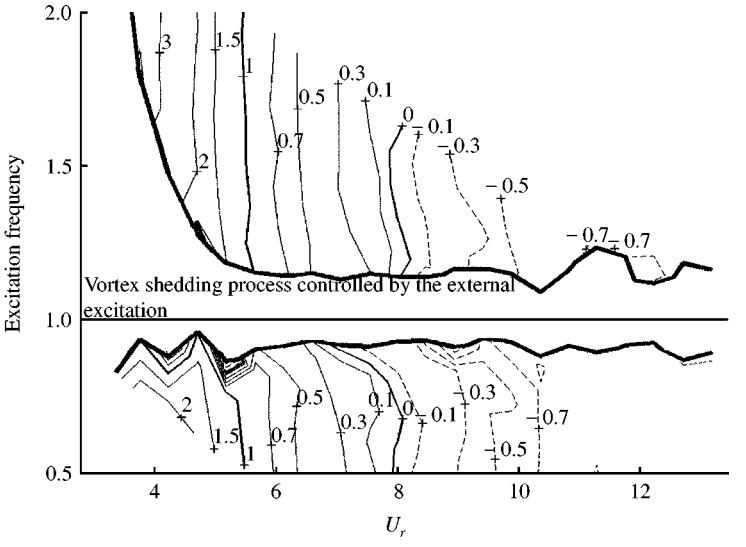

Figure 12. Contours of C_a at the VIV frequency, f_{osc} for 2 cm support motion amplitude, as a function of reduced velocity $U/(f_0 D)$ and external excitation frequency normalized by the mean oscillation frequency for undisturbed VIV, f_{osc} (see Figure 4(b) to see f_{osc} as a function of reduced velocity). The very thick lines show the limits for the region where the external excitation controls the oscillation frequency (see equation (14) for the definition of the region).

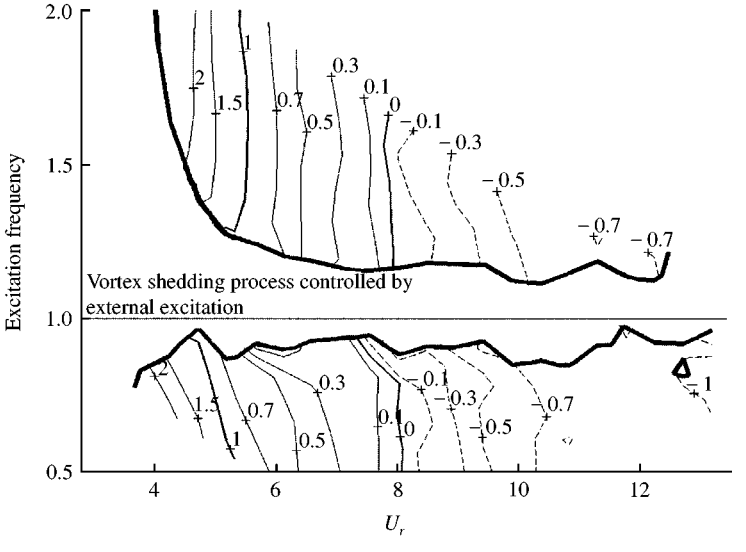

Figure 13. Contours of C_a for 4 cm support motion amplitude. See Figure 12 for detailed information.

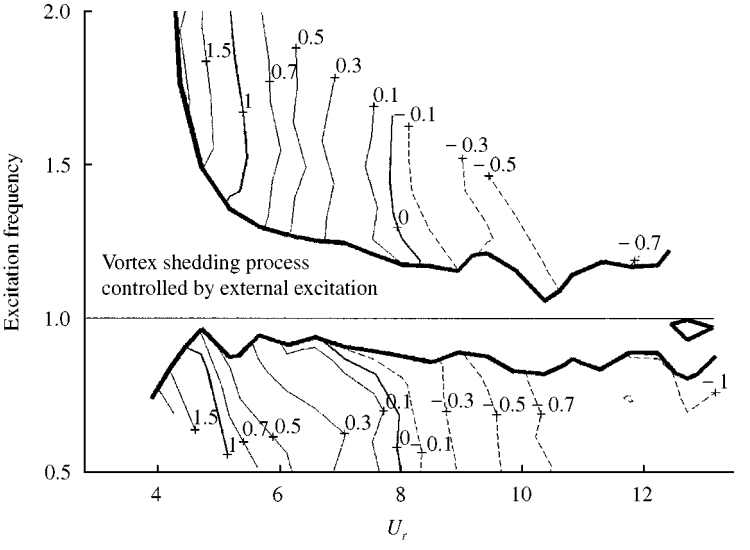

Figure 14. Contours of C_a for 6 cm support motion amplitude. See Figure 12 for detailed information.

which is the dominant cylinder oscillation frequency divided by the support motion frequency. When this frequency ratio is close to 1·0, the support motion controls or reinforces lock-in behavior of the cylinder. When the cylinder has significant VIV response which is different from the support motion frequency, the support motion may interfere with lock-in behavior. In Figures 12–14 the limits $f_{\text{ratio}} = 1{\cdot}1$ (the lower line) and $f_{\text{ratio}} = 0{\cdot}9$ (the upper line) have been chosen to represent the boundary between reinforcement and interference. The added mass coefficients at VIV frequencies in the reinforced or controlled region are discussed in Vikestad (1998). The main result shown in Figures 12–14 is that the added mass coefficient as a function of reduced velocity is similar to the "no support motion" case when the support motion does not control the response. The shift from positive to negative added mass at $U_r = 8$, and the value of $C_a = 1{\cdot}0$ in the region $U_r = 5$–6 are the same as found for a freely vibrating cylinder. When the support motion controls or reinforces the frequency of vortex shedding, the response of the cylinder may be quite different from the free vibration response without support motion. The behavior is quite complex and is discussed in some detail in Vikestad (1998).

5. CONCLUSIONS

From the present results we have found the following.

(i) The added mass coefficient found in free vibration tests for lightly damped cylinders corresponds well to that found by others in driven cylinder tests.

(ii) In the absence of support motion the variation of the added mass from one vibration cycle to the next can be considerable. The variation is least for the reduced velocity range of 4–6.

(iii) In the absence of support motion, the cycle to cycle variation in added mass is closely correlated to a time variation in response frequency, which is interpreted as an added mass-dependent variation in the natural frequency of the cylinder.

(iv) With support motions, the added mass coefficient at the vortex-shedding frequency is a function of reduced velocity and the excitation frequency ratio f_{ex}/f_{osc}.

(v) With support motion, the added mass coefficient is not strongly influenced by the support motion, as long as the vortex-induced response frequency is sufficiently different from the support motion frequency. This region of behaviour has been mapped out in this paper.

ACKNOWLEDGEMENTS

This paper was extracted from the doctoral dissertation of the first author. Financial support for the work was given by The Norwegian Research Council (NFR) through the "Growth Point Centre on Hydroelasticity" at NTNU, by the Faculty of Marine Technology at NTNU, by SINTEF Civil and Environmental Engineering, and by the Joint Industry Project on Deep Water Analysis Tools—"DEEPER". The objective of DEEPER is to enhance calculation methods and computational tools for analysis of deep-water marine structures. The project is jointly run by Det Norske Veritas and MARINTEK and sponsored by The Norwegian Research Council, Norsk Hydro, Statoil, Saga Petroleum, Mobil, Petrobras, Aker Engineering, Kværner Oil & Gas, Offshore Design, Brown & Root, J. Ray McDermott, Umoe Technology, ETPM SA, AMECRC and Det Norske Veritas. Professor Vandiver's participation was sponsored by the Office of Naval Research and by a consortium of petroleum industry companies.

References

Anand, N. M. 1985 Free span vibrations of submarine pipelines in steady and wave flow. Dr.ing. thesis. Division of Port and Ocean Engineering, The Norwegian Institute of Technology.

Gopalkrishnan, R. 1993 Vortex-Induced Forces on Oscillating Bluff Cylinders. Sc.D. thesis, Department of Ocean Engineering, MIT, MA, U.S.A., and Department of Applied Ocean Physics and Engineering, WHOI, MA, U.S.A.

Kozakiewicz, A., Sumer, B. M. & Fredsøe, J. 1994 Cross-flow vibrations of cylinder in irregular oscillatory flow. ASCE *Journal of Waterway, Port, Coastal, and Ocean Engineering* **120,** 515–534.

Sarpkaya, T. 1979 Vortex-induced oscillations — a selective review. *Journal of Applied Mechanics* **46,** 241–258.

Sumer, B. M. & Fredsøe, J. 1997 *Hydrodynamics Around Cylindrical Structures*, pp. 358–363. Singapore: World Scientific.

Vandiver, J. K. 1993 Dimensionless parameters important to the prediction of vortex-induced vibration of long, flexible cylinders in ocean currents. *Journal of Fluids and Structures* **7,** 423–455.

Vikestad, K., Larsen, C. M. & Vandiver, J. K. 1997 Experimental study of excited circular cylinder in current. In *Proceedings of the 16th International Conference on Offshore Mechanics and Arctic Engineering*, Yokohama, Japan, pp. 231–240. New York. ASME.

Vikestad, K. 1998 Multi-frequency response of a cylinder subjected to vortex shedding and support motions. Dr.ing. thesis. Department of Marine Structures, Norwegian University of Science and Technology.